Author Manuscript

Author Manuscript

Author Manuscript

Author Manuscript

HHS Public Access

Author manuscript

Gene Ther. Author manuscript; available in PMC 2014 October 01.

Published in final edited form as:

Gene Ther. 2014 April ; 21(4): 387–392. doi:10.1038/gt.2014.9.

Gene transfer of arginine kinase to skeletal muscle using adeno-associated virus

Sean C. Forbes, PhD[1], **Lawrence T. Bish, MD/PhD**[2], **Fan Ye, PhD**[1], **Janelle Spinazzola**[3], **Celine Baligand, PhD**[4], **Daniel Plant**[5], **Krista Vandenborne, PT, PhD**[1], **Elisabeth R. Barton, PhD**[3], **H. Lee Sweeney, PhD**[2], and **Glenn A. Walter, PhD**[4]

[1]Department of Physical Therapy, University of Florida, Gainesville, FL

[2]Department of Physiology, University of Pennsylvania, Philadelphia, PA

[3]Department of Anatomy and Cell Biology, University of Pennsylvania, Philadelphia, PA

[4]Department of Physiology and Functional Genomics, University of Florida, Gainesville, FL

[5]Advanced Magnetic Resonance Imaging and Spectroscopy Facility, University of Florida, Gainesville, FL

Abstract

In this study we tested the feasibility of non-invasively measuring phosphoarginine (PArg) after gene delivery of arginine kinase (AK) using an adeno-associated virus (AAV) to murine hindlimbs. This was achieved by evaluating the time course, regional distribution, and metabolic flux of PArg using ^{31} phosphorus magnetic resonance spectroscopy (^{31}P-MRS). AK gene was injected into the gastrocnemius of the left hindlimb of C57Bl10 mice (age 5wk, male) using self-complementary AAV, type 2/8 with desmin promoter. Non-localized ^{31}P-MRS data were acquired over nine months after injection using 11.1-T and 17.6-T Bruker Avance spectrometers. In addition, ^{31}P 2-D chemical shift imaging and saturation transfer experiments were performed to examine the spatial distribution and metabolic flux of PArg, respectively. PArg was evident in each injected mouse hindlimb after gene delivery, increased until 28 weeks, and remained elevated for at least nine months ($p<.05$). Furthermore, PArg was primarily localized to the injected posterior hindimb region with the metabolite being in exchange with ATP. Overall, the results show the viability of AAV gene transfer of AK gene to skeletal muscle, and provide support of PArg as a reporter that can be utilized to non-invasively monitor the transduction of genes for therapeutic interventions.

Users may view, print, copy, download and text and data- mine the content in such documents, for the purposes of academic research, subject always to the full Conditions of use: http://www.nature.com/authors/editorial_policies/license.html#terms

Corresponding Authors: Sean C. Forbes, PhD, Box 100154, UFHSC, Department of Physical Therapy, University of Florida, Gainesville, FL 32610, Ph.: (352) 273-6111, Fax: (352) 273-6109, scforbes@ufl.edu. Glenn A. Walter, Ph.D., P.O. Box 100274, Department of Physiology and Functional Genomics, University of Florida, Gainesville, FL 32610, Ph: (352) 392-0551, Fax: (352) 846-0270, glennw@ufl.edu.

Conflict of interest

The authors have no competing financial interests in relation to the work described.

Author Manuscript Author Manuscript Author Manuscript Author Manuscript

Keywords

^{31}Phosphorus magnetic resonance spectroscopy (^{31}P-MRS); gene reporter; arginine kinase; phosphoarginine; creatine kinase; phosphocreatine; skeletal muscle

Introduction

Evaluating gene therapies targeted at treatment of skeletal muscle diseases frequently relies on histological analysis from tissue extracts or muscle biopsies to determine the extent to which regions have been transduced.[1–3] However, a number of non-invasive approaches have shown promise in detecting reporter genes with the potential to obtain longitudinal measures within the same animal or human over time, including optical imaging[4, 5], positron emitting radioisotopes[6], and magnetic resonance imaging (MRI) and spectroscopy (MRS)[7]. MRI-based approaches offer high spatial resolution, and include administration of paramagnetic compounds to alter T_1 contrast (e.g., gadolinium), superparamagnetic and ferromagnetic agents that enhance T_2 and T_2* (e.g., iron oxide particles)[8], and chemical exchange saturation transfer (CEST) based reporter genes.[7, 9] In addition, MRS has been utilized to detect metabolites of gene products. For example, ^{31}phosphorus MRS (^{31}P-MRS) was used to measure the creatine kinase (CK) activity after CK transgenic overexpression[10] and virally mediated gene transfer to the liver.[11, 12]

While MR gene reporter applications to skeletal muscle have generally been limited in the literature, one promising method involves the viral-mediated gene transfer of arginine kinase (AK) into mammalian muscle to result in the production of phosphoarginine (PArg), which can be detected using ^{31}P-MRS.[13] AK is typically found in invertebrates and catalyzes the rephosphorylation of ADP to ATP at the cost of PArg (Eq. 1), and CK is the functionally similar enzyme of vertebrates with phosphocreatine (PCr) as the phosphate donor (Eq. 2). The gene delivery of AK is ideally suited to act as a reporter gene as it provides a unique MR signal against a mammalian background, its coding sequence is small enough to be expressed with therapeutic genes, and it does not appear to interfere with normal tissue function.[13]

$$\mathrm{PArg}+\mathrm{ADP}+\mathrm{H}^{+} \leftrightarrow \mathrm{ATP}+\mathrm{Arg} \quad \text{Eq. (1)}$$

$$\mathrm{PCr}+\mathrm{ADP}+\mathrm{H}^{+} \leftrightarrow \mathrm{ATP}+\mathrm{Cr} \quad \text{Eq. (2)}$$

In a previous study, delivery of AK to skeletal muscle of mice hindlimbs was performed using an adenovirus.[13] However, in order to expand on the potential application of AK gene delivery, in this study we tested the feasibility of using a self-complementary adeno-associated virus (scAAV) to deliver the AK gene with production of PArg monitored over time with ^{31}P-MRS. Using an AAV for delivery is expected to improve biosafety, reduce immune response and toxicity, and increase long-term expression resulting in improved efficacy for *in vivo* use compared to an adenovirus.[14–17] Furthermore, we determined the time course of PArg accumulation, regional distribution using ^{31}P 2-D chemical shift

Author Manuscript Author Manuscript Author Manuscript Author Manuscript

imaging, and enzyme activity of AK and CK using ^{31}P-MRS saturation transfer experiments.

Results

In this study AK gene was delivered to the gastrocnemius muscle of mice using, self-complementary (sc) AAV type 2/8 with desmin promoter, and PArg, PCr, inorganic phosphate (P_i), ATP, and intracellular pH (pH_i) were monitored using ^{31}P-MRS over nine months after injection. In the posterior hindlimbs in which the AK gene was delivered, PArg was evident in each of the mice (n=5) as measured by ^{31}P-MRS (Fig. 1). Consistent with the ^{31}P-MRS data, the existence of AK in the injected gastrocnemius muscle was confirmed using immunoblotting. On the other hand, PArg was not evident in the contralateral limb, nor was AK detected in the contralateral limb using immunoblotting (Fig. 1).

In the hindlimb in which the AK gene was delivered, PArg was evident after one week, increased ($p<0.05$) until 28 weeks after gene delivery, and then remained elevated for at least 37 weeks (Fig. 2). The presence of PArg was evident as a distinct peak in the ^{31}P-MRS spectra in each injected mouse hindlimb eight weeks after gene delivery (Fig. 1). During the initial four weeks following gene delivery, the PArg peak was typically evident as a "shoulder" on the PCr peak or a separate small peak that stemmed from the PCr peak. These peaks were analyzed in the time domain using prior knowledge of the relative peak positions (PCr and PArg separated by 0.44 ppm); using this method we were able to discriminate the PCr and PArg peaks. Fitting both PCr and PArg reduced the residuals and improved the fitting of the spectra in the limbs with AK gene delivered compared to only fitting the PCr peak, providing evidence that PArg was in the muscle at least as early as one week.

The transgene delivery of AK and the subsequent increase of PArg did not appear to affect PCr or P_i concentration or pH_i of the muscle over time, with these measures remaining similar throughout the nine months (Table 1). Compared to the limb with AK gene delivered, the contralateral limb was observed to have a greater ($p=0.04$) concentration of PCr (34.2±4.8 vs. 26.9±1.5 mM), with a similar concentration of P_i (6.2±2.5 vs. 6.0±1.3 mM) and pH_i (7.10±0.06 vs. 7.13±0.08). The contralateral limb of the mice with AK gene delivery was similar ($p>0.05$) to the control wild-type hindlimbs for PCr (33.1±3.3 mM), P_i (4.30± 3.1 mM), and pH_i (7.16±0.16). Furthermore, using localized 2-D ^{31}P chemical shift imaging, PArg was shown to be localized to the injected posterior hindlimb region, and was not evident in deeper regions of the lower hindlimb (Fig. 3).

Saturation transfer experiments

Unidirectional rates and fluxes for PCr → ATP, PArg → ATP, and P_i → ATP in hindlimb muscles of mice after AK gene transfer were estimated using saturation transfer experiments. The measures of reaction fluxes were based on ^{31}P-MRS measures of PCr and PArg at equilibrium and under γ-ATP saturation conditions, as well as with estimates of $T1'$ of PCr, PArg, and P_i. $T1'$ was calculated to be similar ($p>0.05$) in PCr (1.07±0.27 s), PArg (1.02±0.43 s) and P_i (1.06±0.25 s) at 17.6 T.

Author Manuscript Author Manuscript Author Manuscript Author Manuscript

The saturation transfer experiments revealed that PArg was in chemical exchange with ATP, with the rate constant being several-fold lower in the AK than the CK reaction (Table 2). Together with a lower concentration of PArg relative to PCr, the overall flux through the AK reaction was less ($p<0.05$) than through the simultaneous CK reaction (Fig. 4; Table 2). In addition, the fluxes for $P_i \rightarrow$ ATP in hindlimb muscles were observed to be similar ($p>0.05$) in mice after AK gene transfer 1.03±0.37 $mM*s^{-1}$) and in controls (1.02±0.21 $mM*s^{-1}$).

Discussion

In this study we tested the viability of using recombinant scAAV gene transfer of AK gene to skeletal muscle of mice at five weeks of age. The main findings of this study were that: 1) AK gene was successfully delivered to muscle as detected by PArg in ^{31}P spectra and AK in tissue with immunoblotting; 2) an increase of PArg accumulation was observed non-invasively up to 28 weeks, then levels were maintained until at least nine months; 3) PArg was primarily localized in the posterior hindlimb, proximal to the gene delivery injection site; and 4) PArg was in chemical exchange with ATP, with the flux through this reaction being less than through the simultaneous creatine kinase reaction. Collectively, the results support that AAV delivery of the AK gene is effective in providing a gene reporter that can be non-invasively monitored using MR in murine models.

Function of AK

AK is typically found in invertebrates, while CK provides a similar function in mammalian muscle; although there are invertebrates in which both AK and CK have been observed to co-exist in the same cells, such as in the starlet sea anemone Nematostella vectensis.[18] In this study we observed both PCr and PArg simultaneously in the mouse hindlimb in the region of AK gene delivery, with lower rate constants and overall flux at rest through the AK than the CK reaction (Table 2). Consistent with this, Ellington (1989) observed the equilibrium constant of AK to be ~13% of the CK reaction *in vitro* using both enzymatic analysis and ^{31}P-MRS saturation experiments.[19] Furthermore, during one hour of muscle ischemia in a previous study, PCr was depleted to a greater extent (77%) than PArg, (50%) consistent with a reduced equilibrium constant.[13] The similar $P_i \rightarrow$ ATP flux observed between the hindlimb injected with AK gene and controls suggests that net ATP synthesis rate was similar between groups, although the factors that contribute to this measure are not easily interpreted and include contributions from both glycolytic and oxidative sources.[20] Furthermore, with PArg concentration elevated, PCr concentration reduced, and no change in total PArg and PCr in the hindlimbs with AK gene transfer compared to controls, this may be expected to have implications for energy balance under certain conditions. As a result of the higher equilibrium constant of the CK reaction, a primary function of the CK reaction is expected to be the maintenance of ATP levels at the onset of muscle of contractions and during burst activity, while PArg may provide an additional ATP buffer to skeletal muscle, particularly under low PCr and ATP levels. Therefore, the AK reaction would be expected to play a relatively greater role during fatiguing and acidic conditions.[13, 19] As a result, it is possible that AK gene transfer could provide a viable therapeutic approach in ischemic states, perhaps in a similar manner, but possibly to a greater extent, than that observed

Author Manuscript Author Manuscript Author Manuscript Author Manuscript

previously with administration of cyclocreatine.[21–24] Overall, the persistent flux observed through the AK reaction in this study provides support that PArg is in exchange with ATP and this reaction is metabolically active at rest in the mice.

Delivery of AK gene using AAV

The combination of scAAV serotype 2/8 with desmin reporter used in this study was anticipated to result in an efficient and safe transgene delivery to skeletal muscle. AAV has emerged as a safe form of gene delivery with a minimal cellular immune response, since it does not efficiently transduce antigen-presenting cells.[17, 25, 26] Furthermore, AAV has been shown to achieve stable forms of gene expression of up to four years in human subjects[27], and has been widely utilized in a number of clinical studies targeting various tissues, including skeletal muscle in treating dystrophies.[1, 28] In a previous study, PArg was monitored in mice with ^{31}P-MRS after delivery of AK gene using an adenovirus.[13] In that study, the mice were injected at the neonatal stage (1–3 days of age) with a cytomegalovirus (CMV) promotor. The gene transfer at a younger age in that study may have contributed to greater PArg accumulation compared to the present study. However, the adenovirus vector utilized in that study may have limited applicability due to the potential of activating an innate immune response[29] and developing neutralizing antibodies that may block vector readministration.[30] On the other hand, although immune responses were not directly measured in this study, the results show the feasibility of using an AAV delivery of AK gene, which is expected to improve efficacy for *in vivo* use.[14–16] While the results of this study are encouraging, there are obstacles remaining before AAV AK gene delivery could be used in combination with therapeutic interventions, particularly in humans. Challenges include optimizing delivery methods to a greater number of muscles/tissues and avoiding or minimizing an immune response, particularly when moving to larger animal models and in humans. In order to improve distribution, other methods should be investigated, such as systemic delivery methods [31], perhaps in combination with a skeletal muscle ischemia intervention[32].

A number of AAV serotypes have been effectively utilized in skeletal muscle, including the AAV2/8 serotype used in this study. AAV2/8 transduces both Type I and II skeletal muscle fibers efficiently with minimal inflammatory and immune responses in mice.[26] In wild-type mice, six AAV serotypes (AAV2/1, 2, 2/5, 2/7, 2/8 and 2/9) were compared, and AAV2/8 was shown to have the highest transgene expression for muscle-directed gene therapy, with no immune cell response identified.[33] In addition, AAV2/8 effectively delivered microdystrophin and demonstrated restoration of dystrophin in a beagle-based dystrophic dog model, CXMDj.[33] Therefore, there is considerable support for AAV serotype 2/8 being effective for transgene delivery to skeletal muscle.

In this study, a desmin promoter was used with the AAV delivery. Desmin is an intermediate filament located at the periphery of the Z-disks of striated muscle, and has been shown to contribute to the structural integrity and function of muscle.[34] When compared to CMV, alpha-myosin heavy chain (α-MHC), myosin light chain 2(MLC-2) and cardiac troponin C (cTnC) promoters, desmin promoter with a myocyte specific enhancer factor 2 (MEF2) and a MyoD enhancer element showed the greatest expression of LacZ following

Author Manuscript Author Manuscript Author Manuscript Author Manuscript

IV administration of rAAV2/9-mediated gene delivery in skeletal muscle of newborn mice.[35] Also, human desmin promoter matched the activity of human CMV (hCMV) promoter with lentiviral vector delivery to hindlimb skeletal muscle of neonatal mice, with the desmin promoter providing several fold greater expression than the muscle-specific human muscle CK promoter.[36] Furthermore, desmin promoter was utilized as a muscle specific promoter in the effective delivery and restoration of dystrophin in 1–5% of the myofibers of the injected hind limb of *mdx* mice.[37]

Time course of accumulation of PArg after rAAV delivery

In this study we observed that PArg was evident within one week, peaked at 28 weeks, and was maintained until at least nine months. Although it is not possible to determine whether the rate of increase in PArg was limited by AK activity or arginine availability with the measures that we obtained in this study, the presence of PArg confirms AK gene expression. Furthermore, AK expression was observed with immunoblotting. The time course of protein expression has been shown to be highly dependent on a number of factors, including AAV serotype, tissue, and species.[38] In this study scAAV vectors were utilized, which packages a double-stranded genome and eliminates the need for complementary strand synthesis.[39, 40] Although scAAV has the drawback that the size of the DNA packaging capacity of the expression cassette is half of the traditional single-stranded AAV (ssAAV), scAAV offers the advantage of faster onset and greater expression than ssAAV vectors in muscle.[40] Consistent with a rapid onset of AK expression, we observed evidence of PArg accumulation within one week using ^{31}P-MRS. In a previous study comparing scAAV and ssAAV transgene delivery to the tibialis anterior in mice, strong expression was observed after one week using scAAV but minimal expression was noted in ssAAV using florescence.[41] In that study, the transgene expression using scAAV reached a plateau by six weeks and maintained a high level for the 6 months duration of the experiment, whereas the transgene expression of ssAAV increased slowly by six weeks and continued to increase until at least 6 months; at the end of six months, the scAAV had 15 fold greater expression than ssAAV.[41] Similarly, using scAAV has been shown to result in expression of the myocardium within four days in small animals[42] and one week of canines.[39] Overall, the combination of scAAV serotype 2/8 with desmin reporter used in this study was shown to be effective in the transgene delivery of AK to skeletal muscle of mice.

In summary, the results of this study support the use of ^{31}P-MRS to monitor PArg non-invasively in mammalian muscle, providing a robust way of evaluating the transduction of gene expression. The distinct resonance frequency of PArg provides a unique signal that can be non-invasively evaluated. In this study we exploited high-field strength MR to further enhance chemical shift differences between PCr and PArg and 2D ^{31}P chemical shift imaging provided spatial information of gene transduction. Although MRI measures of reporter genes have the potential to provide high spatial resolution, these methods are often affected by non-specific coinciding variables associated with vector delivery or disease process, such as inflammation.[8] Overall, the results of this study using ^{31}P-MRS show the viability of AAV gene transfer of AK gene to skeletal muscle of mice, and provide support for use as a gene reporter to non-invasively monitor the delivery of genes for therapeutic interventions.

Author Manuscript Author Manuscript Author Manuscript Author Manuscript

Materials and Methods

Animals—Wild-type C57BL/10ScSn mice (male; n=10) were obtained from Jackson Laboratories (Bar Harbor, Maine), and thereafter maintained in-house in an Association for Assessment and Accreditation of Laboratory Animal Care (AAALAC) approved facility with a 12-hour light:dark cycle (72°F, 42% humidity) and free access to food and water. The experimental protocol was approved by the institutional animal care and use committee (IACUC) at the University of Florida.

Injections—Direct intramuscular injection of replication deficient AAV encoding for the AK gene into the hindlimb of mice was performed as previously described.[17, 43] Specifically, scAAV, type 2/8 with desmin promoter (5.0×10^{10} particles/leg) were delivered with 80 μl of phosphate buffered saline (PBS) to the left gastrocnemius of the mice. Five mice received the injection with encoding for the AK gene, and the remaining five mice served as controls.

Magnetic resonance spectroscopy

The mice were anesthetized using an oxygen (1L/min) and isoflurane mixture (3% isoflurane) and maintained with 1% isoflurane in O_2 delivered through an anesthesia mask with a scavenger valve for the duration of the MR procedure. Body temperature was maintained through an MR compatible heating system that provided heated air into the bore of the magnet, and respiratory rate was monitored for the duration of the scans (Small Animal Instruments, Inc. (SAII), Stony Brook, New York, USA).

^{31}P-MRS data were acquired using 11.1-T 40 cm horizontal bore and 17.6-T 89 mm vertical bore systems with Bruker Avance spectrometers (Paravision, Version 3.02, Bruker Corporation, Billerica, Massachusetts, USA). Mice were positioned prone with the hindlimb being extended, and an oblong transmit/receive ^{31}P surface coil (6 mm × 12 mm) centered on the posterior region of the lower hindlimb (11.1T, 190.6 mHz: built in-house; 17.6T, 303.7 mHz: Doty Scientific, Columbia, South Carolina, USA). Also, a ^{1}H tuned surface coil was placed adjacent to the hindlimb for localized shimming of the posterior hindlimb region. ^{31}P data were collected at weekly intervals for the initial four weeks after gene delivery, then at 2–6 week intervals up to 37 weeks using an 11.1-T (TR 2 s, 256 NSA, 2048 data points, 8kHz sweep width) or a 17.6-T (TR 2 s, 256 NSA, 8096 data points, 10kHz sweep width) system. ^{31}P-MRS data of the contralateral limb was acquired at 28 weeks after AK gene transfer. Furthermore, ^{31}P-MRS data from a hindlimb of the non-injected control mice were acquired at 30 weeks of age.

In addition, at 16 weeks after gene transfer, ^{31}P 2-D chemical shift imaging (CSI) was acquired (8×8 matrix, 10–15 mm FOV, 3 mm axial slice thickness, TR 2 s, 32 NSA, 4096 data points, spectral width 10080.6Hz) at 11.1-T to examine the spatial distribution of PArg in the mouse hindlimb. In addition, we performed ^{31}P saturation transfer experiments at 17.6-T in the injected hindlimb after 28–32 weeks of gene delivery using selective saturation of γ-ATP for 2, 4, 6, and 8 s (gauss pulse shape, pulse length 12000 μsec, with an interpulse delay of 200 μsec, power 1.2 μT). The spectra were acquired using 32 averages with a TR of

Author Manuscript Author Manuscript Author Manuscript Author Manuscript

10 s (excitation pulse shape pb32, 50 μsec). Spectra were also acquired with a saturation frequency that mirrored the difference in frequency of the center of PCr and PArg and γ-ATP (665±8 Hz) to account for any radiofrequency (RF) bleeding.

Magnetic resonance spectroscopy analysis

Non-localized ^{31}P-MRS—The relative concentration of P_i, PCr, PArg, and γ-, α-, and β-ATP were quantified using the Advanced Method for Accurate, Robust and Efficient Spectral (AMARES) fitting algorithm of jMRUI (Version 5.0). This analysis was performed in the time domain with zero and first order phasing, PCr set at 0 ppm for reference, and using estimated starting values (P_i: 4.85 ppm, PCr: 0 ppm, PArg: −0.44 ppm, γ-ATP: −2.49 ppm, α-ATP: 7.5 ppm, β-ATP: −16.1 ppm) and prior knowledge (fixed shift of PArg of 0.44 ppm relative to PCr and Lorentzian line shapes). To account for partial saturation, signal intensities were multiplied by correction factors derived using spectra acquired with a TR of 2 s and 15 s at 11.1-T (PCr, 1.45±0.33; PArg, 1.46±0.36; γ-ATP, 1.33±0.40; P_i, 1.87±0.25) and 17.6-T (PCr, 1.07±0.04; PArg, 1.08±0.04; γ-ATP, 1.08±0.04; P_i, 1.26±0.11). Concentrations of PCr, PArg, and P_i were calculated assuming an ATP concentration of 8.7 mM.[13]

^{31}P 2D-CSI—Analyses of the localized phosphorus spectra were performed using 3DiCSI software (Version 1.9.9).[44] Spectra were viewed in an 8×8 matrix, then zero-filled (16×16), phased, and the corresponding free induction decays (FID) within the regions of interest (i.e., posterior and medial compartment) were exported and analyzed using the jMRUI software (Version 5.0). Analyses of the spectra were performed by aligning the spectra, setting the PCr peak to 0 ppm, and summing the spectra within each compartment to produce a single spectrum.

Saturation transfer experiments

The rates of transfer of phosphate from PCr and PArg to γ-ATP were estimated by saturation transfer using a pseudo-first-order exchange model.[45, 4647] The exchange rate constants of PCr and PArg with ATP were calculated based on the equation:

$$k=(Mo-Ms)/(T^{'}*Ms) \quad \text{Eq. (3)}$$

where *k* is a rate constant describing the loss of magnetization due to exchange of saturated spins between PCr or PArg and ATP, T_1' is the apparent longitudinal relaxation time of PCr or PArg, M_S is the steady state phosphate signal under γ-ATP saturation, and *Mo* is the phosphate signal at its equilibrium value. *Ms* was determined by fitting the decay of phosphate signal with saturation time using a monoexponential model, with *Ms* expressed relative to *Mo* measured with the mirror frequency saturation. Also, the exchange rate constant of P_i with ATP was calculated based on the equation[48]:

$$k=(1-Ms/Mo)/(T^{'}) \quad \text{Eq. (4)}$$

Estimation of T_1' of PCr, PArg, and P_i was accomplished by varying TR (0.8, 1.3, 1.8, 2.3, 3.3, 5.3, 7.3, and 10.3 s) and fitting with a mono-exponential model. Following the

Author Manuscript Author Manuscript Author Manuscript Author Manuscript

calculation of *k* for PCr, PArg, and P_i the unidirectional flux of ATP synthesis was calculated as the product of *k* and corresponding metabolite concentration using the following equations:

$$Flux\ PCr \rightarrow ATP = k\,[PCr] \quad \text{Eq. (5)}$$

$$Flux\ PArg \rightarrow ATP = k\,[PArg] \quad \text{Eq. (6)}$$

$$Flux\ P_i \rightarrow ATP = k\,[P_i] \quad \text{Eq. (7)}$$

Immunoblotting—Gastrocnemius muscles of the injected and contralateral limbs were performed by dissecting, freezing in liquid nitrogen, and storing in −80°C. Upon removal from storage, the muscles were crushed on dry ice, tendons removed, and homogenized in a radioimmune precipitation assay (RIPA) buffer (10 μl/mg of dry muscle weight). Tissue homogenates were centrifuged to pellet debris and the total protein was measured in the supernatant using a Bradford procedure (Bio-Rad protein assay; Bio-Rad Laboratories, Hercules, California). Protein from each muscle were separated by gel electrophoresis (SDS-PAGE) and transferred to Polyvinylidene fluoride membranes (Immobilon-P; Millipore, Bedford, MA). Membranes were incubated in a blocking buffer and stirred for 90 minutes, and then incubated overnight at 4°C with primary antibody diluted in 5% dried milk with TTBS. Primary antibodies included those for AK (1:10000) and tubulin (1:3000). After washes and exposure to secondary antibodies recognizing rabbit (LI-COR Biosciences, Lincoln, NE, USA), specific bands were visualized by film using Image Quant LAS 4000 (GE Healthcare Biosciences, Pittsburg, Pennsylvania).

Statistics

Longitudinal changes were compared using a one-way repeated measures ANOVA (Prism Software, GraphPad, v6.0b). Comparisons between AK and CK fluxes, hindlimb regions, and hindlimb with AK gene delivered versus contralateral hindlimbs and controls were evaluated using paired T-tests (Prism Software, GraphPad, v6.0b). Statistical significance was defined as a p-value less than or equal to 0.05. Data are reported as mean (SD) in the text and tables and mean (SEM) in the figures.

Acknowledgments

This study was supported by National Institutes of Health (P01 HL59412 to GAW), Muscular Dystrophy Association Development Grant (175552 to SCF), and the National High Magnetic Field Laboratory. We thank Huadong Zeng, PhD of the Advanced Magnetic Resonance Imaging and Spectroscopy (AMRIS) facility in the McKnight Brain Institute of the University of Florida.

References

1. Mendell JR, Rodino-Klapac LR, Rosales XQ, Coley BD, Galloway G, Lewis S, et al. Sustained alpha-sarcoglycan gene expression after gene transfer in limb-girdle muscular dystrophy, type 2D. Ann Neurol. 2010; 68(5):629–638. [PubMed: 21031578]

Author Manuscript Author Manuscript Author Manuscript Author Manuscript

2. Wang Z, Storb R, Halbert CL, Banks GB, Butts TM, Finn EE, et al. Successful regional delivery and long-term expression of a dystrophin gene in canine muscular dystrophy: a preclinical model for human therapies. Mol Ther. 2012; 20(5):1501–7. [PubMed: 22692496]

3. Haecker SE, Stedman HH, Balice-Gordon RJ, Smith DBJ, Greelish JP, Mitchell MA, et al. In Vivo Expression of Full-Length Human Dystrophin from Adenoviral Vectors Deleted of All Viral Genes. Hum Gene Ther. 1996; 7(15):1907–1914. [PubMed: 8894682]

4. Weissleder R, Ntziachristos V. Shedding light onto live molecular targets. Nat Med. 2003; 9(1): 123–128. [PubMed: 12514725]

5. Tangney M, Francis KP. In vivo optical imaging in gene & cell therapy. Curr Gene Ther. 2012; 12(1):2–11. [PubMed: 22263919]

6. Gambhir SS, Barrio JR, Phelps ME, Iyer M, Namavari M, Satyamurthy N, et al. Imaging adenoviral-directed reporter gene expression in living animals with positron emission tomography. Proc Natl Acad Sci U S A. 1999; 96(5):2333–2338. [PubMed: 10051642]

7. Gilad AA, Ziv K, McMahon MT, van Zijl PCM, Neeman M, Bulte JWM. MRI Reporter Genes. J Nucl Med. 2008; 49(12):1905–1908. [PubMed: 18997049]

8. Iordanova B, Goins WF, Clawson DS, Hitchens TK, Ahrens ET. Quantification of HSV-1-mediated expression of the ferritin MRI reporter in the mouse brain. Gene Ther. 2012; 20(6):589–96. [PubMed: 22996196]

9. Sherry AD, Woods M. Chemical exchange saturation transfer contrast agents for magnetic resonance imaging. Annu Rev Biomed Eng. 2008; 10:391–411. [PubMed: 18647117]

10. Koretsky AP, Brosnan MJ, Chen LH, Chen JD, Van Dyke T. NMR detection of creatine kinase expressed in liver of transgenic mice: determination of free ADP levels. Proc Natl Acad Sci U S A. 1990; 87(8):3112–3116. [PubMed: 2326269]

11. Li Z, Qiao H, Lebherz C, Choi SR, Zhou X, Gao G, et al. Creatine kinase, a magnetic resonance-detectable marker gene for quantification of liver-directed gene transfer. Hum Gene Ther. 2005; 16(12):1429. [PubMed: 16390274]

12. Auricchio A, Zhou R, Wilson JM, Glickson JD. In vivo detection of gene expression in liver by 31P nuclear magnetic resonance spectroscopy employing creatine kinase as a marker gene. Proc Natl Acad Sci U S A. 2001; 98 (9):5205–5210. [PubMed: 11296261]

13. Walter G, Barton ER, Sweeney HL. Noninvasive measurement of gene expression in skeletal muscle. Proc Natl Acad Sci USA. 2000; 97(10):5151–5155. [PubMed: 10805778]

14. Rabinowitz JE, Samulski J. Adeno-associated virus expression systems for gene transfer. Curr Opin Biotechnol. 1998; 9(5):470–475. [PubMed: 9821274]

15. Konieczny P, Swiderski K, Chamberlain JS. Gene and cell-mediated therapies for muscular dystrophy. Muscle Nerve. 2013; 47(5):649–663. [PubMed: 23553671]

16. Xiao X, Li J, Samulski RJ. Efficient long-term gene transfer into muscle tissue of immunocompetent mice by adeno-associated virus vector. J Virol. 1996; 70 (11):8098–108. [PubMed: 8892935]

17. Gruntman AM, Bish LT, Mueller C, Sweeney HL, Flotte TR, Gao G. Gene transfer in skeletal and cardiac muscle using recombinant adeno-associated virus. Curr Protoc Microbiol. 2013; Chapter 1(Unit 14D)

18. Uda K, Ellington WR, Suzuki T. A diverse array of creatine kinase and arginine kinase isoform genes is present in the starlet sea anemone Nematostella vectensis, a cnidarian model system for studying developmental evolution. Gene. 2012; 497(2):214–227. [PubMed: 22305986]

19. Ellington W. Phosphocreatine represents a thermodynamic and functional improvement over other muscle phosphagens. J Exp Biol. 1989; 143(1):177–194. [PubMed: 2543728]

20. From AHL, Ugurbil K. Standard magnetic resonance-based measurements of the P→ATP rate do not index the rate of oxidative phosphorylation in cardiac and skeletal muscles. Am J Physiol Cell Physiol. 2011; 301(1):C1–C11. [PubMed: 21368294]

21. Wiseman RW, Kushmerick MJ. Creatine Kinase Equilibration Follows Solution Thermodynamics in Skeletal Muscle. J Biol Chem. 1995; 270(21):12428–12438. [PubMed: 7759484]

22. Annesley TM, Walker JB. Energy metabolism of skeletal muscle containing cyclocreatine phosphate. Delay in onset of rigor mortis and decreased glycogenolysis in response to ischemia or epinephrine. J Biol Chem. 1980; 255(9):3924–30. [PubMed: 7372660]

Author Manuscript Author Manuscript Author Manuscript Author Manuscript

23. Osbakken M, Ito K, Zhang D, Ponomarenko I, Ivanics T, Jahngen E, et al. Creatine and cyclocreatine effects on ischemic myocardium: 31P nuclear magnetic resonance evaluation of intact heart. Cardiology. 1992; 80(3–4):184–195. [PubMed: 1511465]
24. Roberts JJ, Walker JB. Feeding a creatine analogue delays ATP depletion and onset of rigor in ischemic heart. Am J Physiol Heart Circ Physiol. 1982; 243(6):H911–H916.
25. Jooss K, Yang Y, Fisher KJ, Wilson JM. Transduction of dendritic cells by DNA viral vectors directs the immune response to transgene products in muscle fibers. J Virol. 1998; 72(5):4212–23. [PubMed: 9557710]
26. Louboutin J-P, Wang L, Wilson JM. Gene transfer into skeletal muscle using novel AAV serotypes. J Gene Med. 2005; 7(4):442–451. [PubMed: 15517544]
27. Manno CS, Chew AJ, Hutchison S, Larson PJ, Herzog RW, Arruda VR, et al. AAV-mediated factor IX gene transfer to skeletal muscle in patients with severe hemophilia B. Blood. 2003; 101(8):2963–2972. [PubMed: 12515715]
28. Stedman HWJ, Finke R, Kleckner AL, Mendell J. Phase I clinical trial utilizing gene therapy for limb girdle muscular dystrophy: alpha-, beta-, gamma-, or delta-sarcoglycan gene delivered with intramuscular instillations of adeno-associated vectors. Hum Gene Ther. 2000; 11(5):777–790. [PubMed: 10757357]
29. Schnell MA, Zhang Y, Tazelaar J, Gao G-p, Yu QC, Qian R, et al. Activation of Innate Immunity in Nonhuman Primates Following Intraportal Administration of Adenoviral Vectors. Mol Ther. 2001; 3:708–722. [PubMed: 11356076]
30. Yang Y, Ehlen Haecker S, Su Q, Wilson JM. Immunology of Gene Therapy with Adenoviral Vectors in Mouse Skeletal Muscle. Hum Mol Genet. 1996; 5(11):1703–1712. [PubMed: 8922997]
31. Bostick B, Ghosh A, Yue Y, Long C, Duan D. Systemic AAV-9 transduction in mice is influenced by animal age but not by the route of administration. Gene Ther. 2007; 14(22):1605–1609. [PubMed: 17898796]
32. Katwal AB, Konkalmatt PR, Piras BA, Hazarika S, Li SS, John Lye R, et al. Adeno-associated virus serotype 9 efficiently targets ischemic skeletal muscle following systemic delivery. Gene Ther. 2013; 20(9):930–938. [PubMed: 23535898]
33. Koo T, Okada T, Athanasopoulos T, Foster H, Takeda Si, Dickson G. Long-term functional adeno-associated virus-microdystrophin expression in the dystrophic CXMDj dog. J Gene Med. 2011; 13(9):497–506. [PubMed: 22144143]
34. Paulin D, Li Z. Desmin: a major intermediate filament protein essential for the structural integrity and function of muscle. Exp Cell Res. 2004; 301(1):1–7. [PubMed: 15501438]
35. Pacak C, Sakai Y, Thattaliyath B, Mah C, Byrne B. Tissue specific promoters improve specificity of AAV9 mediated transgene expression following intra-vascular gene delivery in neonatal mice. Genet Vaccines Ther. 2008; 6(1):13. [PubMed: 18811960]
36. Talbot GE, Waddington SN, Bales O, Tchen RC, Antoniou MN. Desmin-regulated Lentiviral Vectors for Skeletal Muscle Gene Transfer. Mol Ther. 2010; 18(3):601. [PubMed: 19935780]
37. Zhang G, Ludtke JJ, Thioudellet C, Kleinpeter P, Antoniou M, Herweijer H, et al. Intraarterial delivery of naked plasmid DNA expressing full-length mouse dystrophin in the mdx mouse model of duchenne muscular dystrophy. Hum Gene Ther. 2004; 15(8):770. [PubMed: 15319034]
38. Palomeque J, Chemaly ER, Colosi P, Wellman JA, Zhou S, del Monte F, et al. Efficiency of eight different AAV serotypes in transducing rat myocardium in vivo. Gene Ther. 2007; 14(13):989–997. [PubMed: 17251988]
39. Bish LT, Sleeper MM, Brainard B, Cole S, Russell N, Withnall E, et al. Percutaneous Transendocardial Delivery of Self-complementary Adeno-associated Virus 6 Achieves Global Cardiac Gene Transfer in Canines. Mol Ther. 2011; 16(12):1953–1959. [PubMed: 18813281]
40. McCarty DM. Self-complementary AAV Vectors; Advances and Applications. Mol Ther. 2008; 16(10):1648–1656. [PubMed: 18682697]
41. Wang Z, Ma H-I, Li J, Sun L, Zhang J, Xiao X. Rapid and highly efficient transduction by double-stranded adeno-associated virus vectors in vitro and in vivo. Gene Ther. 2003; 10(26):2105–2111. [PubMed: 14625564]

Author Manuscript Author Manuscript Author Manuscript Author Manuscript

42. Andino L, Conlon T, Porvasnik S, Boye S, Hauswirth W, Lewin A. Rapid, widespread transduction of the murine myocardium using self-complementary Adeno-associated virus. Genet Vaccines Ther. 2007; 5(1):13. [PubMed: 18070352]

43. Ye F, Mathur S, Liu M, Borst SE, Walter GA, Sweeney HL, et al. Overexpression of insulin-like growth factor-1 attenuates skeletal muscle damage and accelerates muscle regeneration and functional recovery after disuse. Exp Physiol. 2013; 98(5):1038–1052. [PubMed: 23291913]

44. Zhao Q, Patriotis P, Arias-Mendoza F, Stoyanova R, Brown TR. An interactive software for 3D chemical shift imaging data analysis and real time spectral localization and quantification. Proc Int Soc Mag Reson Med. 2005; 13:2465.

45. Meyer RA, Kushmerick MJ, Brown TR. Application of 31P-NMR spectroscopy to the study of striated muscle metabolism. Am J Physiol. 1982; 242(1):C1–C11. [PubMed: 7058872]

46. Gupta A, Chacko VP, Schar M, Akki A, Weiss RG. Impaired ATP Kinetics in Failing In Vivo Mouse Heart. Circ Cardiovasc Imaging. 2011; 4(1):42–50. [PubMed: 20926788]

47. Nabuurs C, Huijbregts B, Wieringa B, Hilbers CW, Heerschap A. 31P Saturation Transfer Spectroscopy Predicts Differential Intracellular Macromolecular Association of ATP and ADP in Skeletal Muscle. J Biol Chem. 2010; 285(51):39588–39596. [PubMed: 20884612]

48. Larsen RG, Befroy DE, Kent-Braun JA. High-intensity interval training increases in vivo oxidative capacity with no effect on Pi→ATP rate in resting human muscle. Am J Physiol Regul Integr Comp Physiol. 2013; 304(5):R333–R342. [PubMed: 23255590]

Author Manuscript Author Manuscript Author Manuscript Author Manuscript

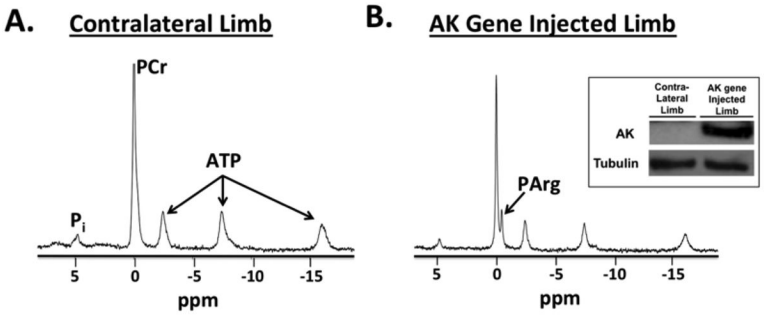

Figure 1.

Example ^{31}P spectrum acquired at 17.6T in the contralateral limb (A) and in the limb injected with arginine kinase (AK) gene (B) acquired at 28 weeks. In the posterior hindlimbs in which the AK gene was delivered, PArg was evident in each of the mice (n=5). Also, AK was confirmed using immunoblotting in the injected gastrocnemius muscle (see insert for example AK and tubulin blots). On the other hand, PArg and AK were not evident in the contralateral limb.

Author Manuscript Author Manuscript Author Manuscript Author Manuscript

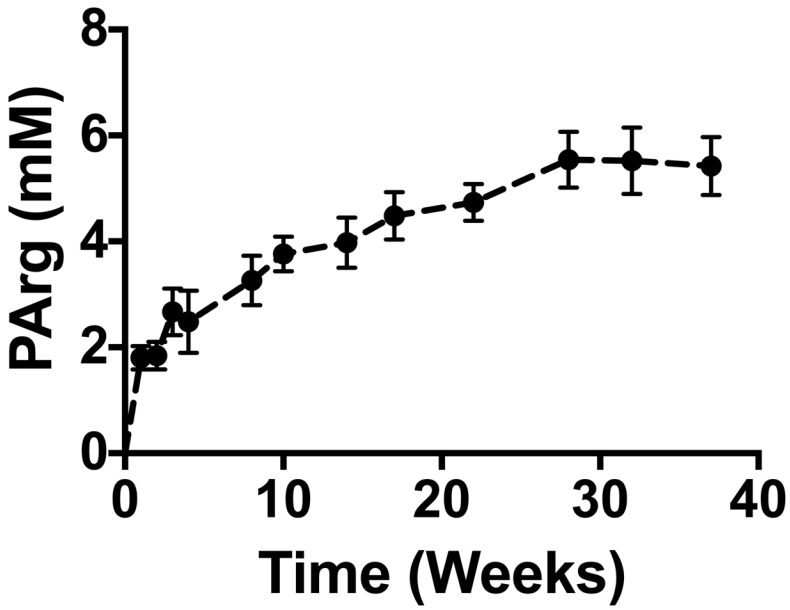

Figure 2.

Time course of phosphoarginine (PArg) changes in the hindlimb muscles after arginine kinase gene delivery. PArg was evident in the spectra of each injected mouse hindlimb, continued to increase until 28 weeks, and remained elevated for at least nine months. Values are expressed as mean±SEM; n=5.

Author Manuscript Author Manuscript Author Manuscript Author Manuscript

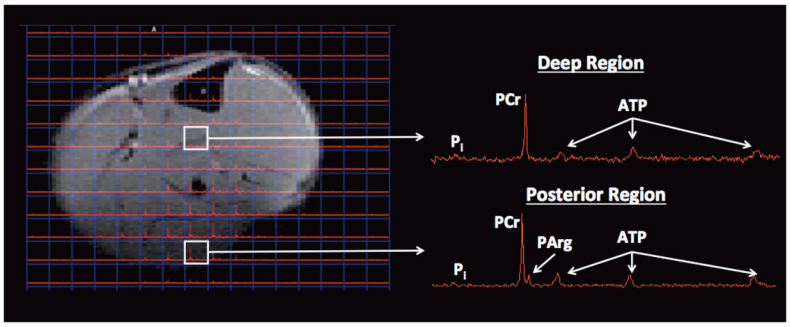

Figure 3.

Phosphoarginine (PArg) was evident in the posterior region of the hindlimb using ^{31}P 2D CSI with an 11.1T MR system, but was not apparent in other regions of the hindlimb, such as in the deeper hindlimb muscles. ^{31}P 2-D chemical shift imaging (CSI) was acquired with an 8×8 matrix, 15×15mm^2 FOV, 3 mm axial slice thickness, and was zero filled to a 16×16 matrix.

Author Manuscript Author Manuscript Author Manuscript Author Manuscript

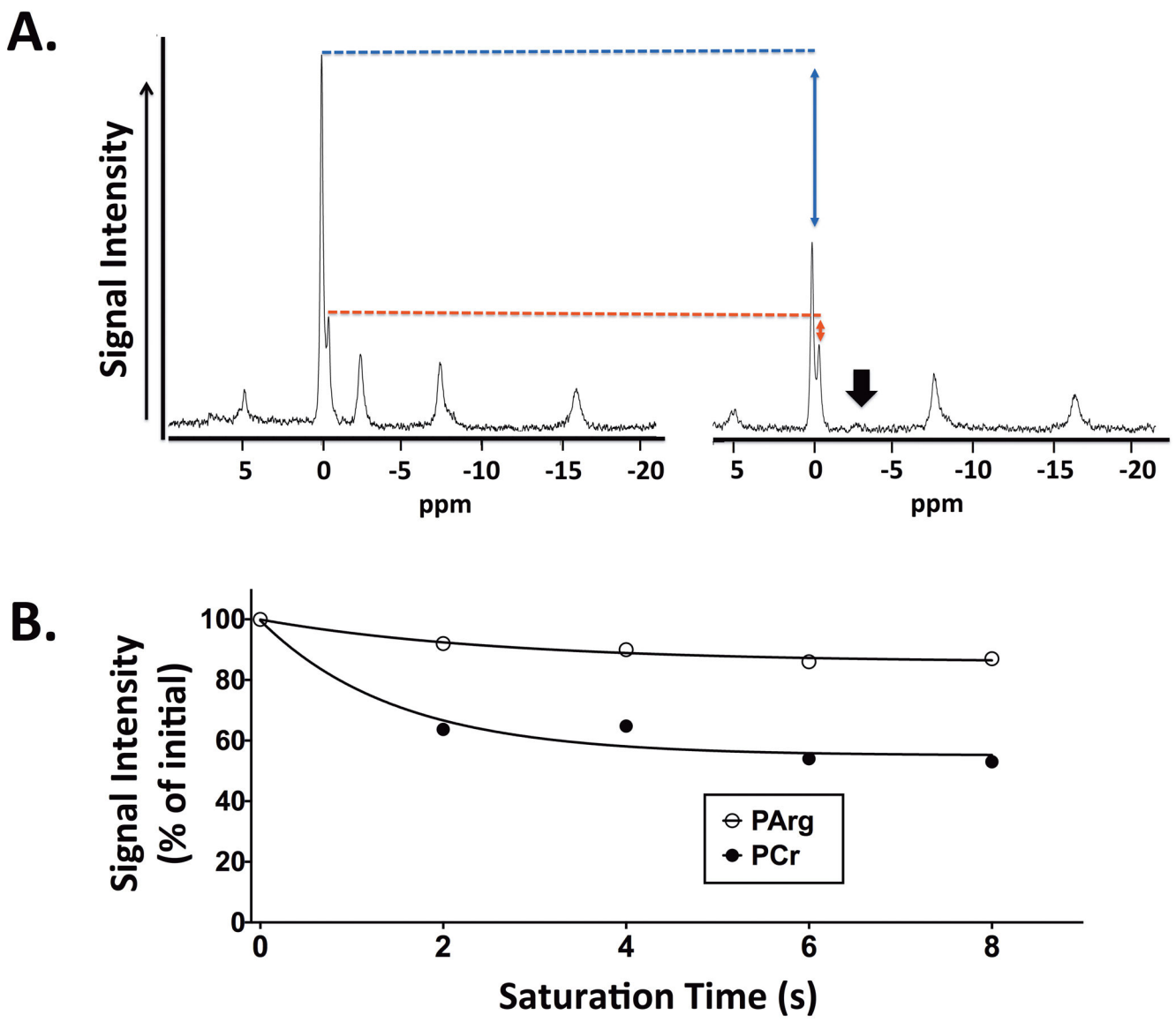

Figure 4.

^{31}P spectra with and without saturation of γ-ATP acquired at 17.6T (A). The saturation transfer experiments revealed that PArg was in chemical exchange with γ-ATP, with the rate of the reaction being less than through the simultaneous creatine kinase reaction (B).

Author Manuscript Author Manuscript Author Manuscript Author Manuscript

Table 1

Concentrations of phosphocreatine (PCr) and inorganic phosphate (P_i) and intracellular pH (pH_i) in the posterior hindlimbs of mice after gene delivery of arginine kinase (AK).

	Week 1	Week 2	Week 3	Week 4	Week 8	Week 10	Week 14	Week 17	Week 22	Week 28	Week 32	Week 37
PCr (mM)	24.8 (1.7)	26.0 (5.1)	27.1 (1.5)	26.0 (5.9)	25.5 (2.2)	23.5 (3.0)	23.9 (1.3)	25.1 (3.4)	27.2 (2.3)	26.9 (1.5)	26.8 (0.7)	25.2 (3.1)
Pi (mM)	6.4 (0.9)	7.2 (0.9)	6.2 (0.6)	6.2 (1.2)	7.2 (0.8)	7.0 (1.0)	7.2 (2.1)	5.2 (1.0)	6.5 (1.2)	6.0 (1.3)	6.5 (1.4)	5.9 (1.6)
pH_i	7.12 (0.04)	7.16 (0.08)	7.12 (0.04)	7.12 (0.06)	7.07 (0.12)	7.09 (0.06)	7.14 (0.10)	7.08 (0.10)	7.10 (0.06)	7.13 (0.08)	7.10 (0.03)	7.09 (0.11)

No significant changes were observed over time in PCr, P_i and pH_i in the hindlimb after AK gene transfer. Values are expressed as mean (SD); n=5.

Author Manuscript

Author Manuscript

Author Manuscript

Author Manuscript

Table 2

Unidirectional rates and fluxes for PCr → ATP and PArg → ATP in hindlimb muscles of mice after arginine kinase (AK) gene transfer

	PCr	PArg
k (s^{-1})	0.47±0.20	0.04±0.05*
Flux (mM^{*} s^{-1})	12.6±5.2	0.17±0.22*

Values are presented as mean±SD.

*Significantly different ($p<0.05$) from PCr k and flux. Values are expressed as mean±SD; n=5.